A Tunable Perceptual Microsystem for Stereo Depth Estimation

Federico Bruccoleri, Silvio P. Sabatini, and Giacomo M. Bisio
PSPC Reseach Group - DIBE, University of Genoa - Via Opera Pia, 11a - 16145 Genova, Italy

Luigi Raffo
DIEE, University of Cagliari - P.zza Armi - 09123 Cagliari, Italy

***Abstract*—The paper presents the design and analyzes the applications of a microsystem to be used for emulating, in real time, early vision tasks, such as stereo depth estimation and motion analysis. All the required computations are based on linear filtering operations with Gabor-like kernels. Full control on the parameters (phase, frequency, and spatial extension) of the kernel can be obtained by introducing a 2nd-order 1-D lattice network that can be mapped with efficiency on an array of simple cells, implemented as analog CMOS VLSI circuits, using continuously adjustable transconductors.**

I. Introduction

Analog approaches to the hardware implementation of machine vision systems can be very effective as far as real-time performance, size, and power consumption are concerned, but machine functionality, with regard both to the variety of tasks to be performed, and to the conditions of application, can be hindered by the limited flexibility and lack of programmability of analog circuits. A solution to this problem can be searched through a systematic approach to the sensorial/perceptual computations, that goes from proper model/algorithmic formulations, through adequate architectures based on flexible primitives, to efficient VLSI circuital solutions.

In this paper, we present the architectural and the circuital solutions for the implementation of visual microsystems to be used in the emulation of early vision tasks. The single-chip microsystem is characterised by three levels of adaptability: (i) a variety of algorithms (e.g., stereo depth estimation, texture and motion analysis) can be specified in terms of convolutions with spatial Gabor-like filters; (ii) Gabor-like kernels of variable phase can be obtained as linear combination of the same recurrent filter response; (iii) the frequency and the spatial extension of the Gabor-like kernel can be controlled by analog tunable circuits. In particular, we propose and analyse an analog CMOS implementation of a tunable computational engine based on linear continuously adjustable transconductors to be used as a front-end module of a vision system. In this way, we can reach real-time computational efficiency in the measuring process on the visual space, by using a coarse-to-fine strategy to take into account that different characteristics of an image reveal themselves at different levels of resolution [1]. These operations are typical in computer vision algorithms where each image is analysed through a bank of filters of different size and tuned to different spatial frequencies (multichannel approach) [2] [3]. With reference to such multi-scale algorithms and on the ground of the neurophysiological and psychophysical findings in natural vision [4] [5], a VLSI system able to perform, on the same substrate, multichannel analysis of the sensed image is really desirable, and may have challenging impact on the functionality and performance of artificial vision microsystems. To validate the approach, experimental results on stereo depth estimation are presented.

II. The perceptual microsystem

A. Lattice networks for early vision tasks

Early vision tasks concern the analysis of visual information by the decomposition of the input image into coherent components that can be independently characterized [6]. Thus, the first stages of a vision system should be able to extract quickly and efficiently the *salient* information in the image, represented in natural scenes by lines, edges, textures, stereo cues, velocity fields, etc. Various computational vision models can make use of Gabor-like functions as localized spatial filters or as basic functions for image transformations [5] [7]. These computations can be formalized in term of spatially continous linear operators specified in differential and/or integral form [8][9] [1]. We consider a discrete 1-D form of these operator mapped on a network of interactive nodes (i.e. lattice network), with various degree of locality. Every node of the lattice network is excited by the visual signal $s(n)$ and is connected to the nearest and the next nearest neighbor nodes [10]. The functionality of this lattice network can be described by the following second-order linear difference equation in the excitation level $e(n)$:

$$A_2e(n-2) - A_1e(n-1) + e(n) - A_1e(n+1) + \\ +A_2e(n+2) = s(n) \qquad (1)$$

where A_i are coefficients describing the interactions among the nodes of the 1-D lattice network. According to [11], for points $\underline{A} = (A_1, A_2)$ inside the elliptic domain $D = \{(A_1, A_2) : A_1^2 < 4A_2 - 8A_2^2\}$ (see Fig. 1), the 1-D lattice network is characterised by a stable impulse response

Corresponding author Federico Bruccoleri, 39-10-3532794, fax 39-10-3532795, pspc@dibe.unige.it, http://dibe.unige.it/department/micro/pspc/home.html.

This work was partially supported by the *CEC- Esprit BR Project CORMORANT-8503*, by the *University of Genoa Project "Strutture Fisiche per la Percezione e l'Elaborazione"* and by *ASI Project "Microsistemi Ottici per la Robotica Spaziale"*.

$h^{(2)}(n)$ of the following type:

$$h^{(2)}(n) = Ce^{-|n|/\lambda}((1+e^{-2/\lambda})sin(\omega_0)cos(\omega_0 n) + \\ +(1-e^{-2/\lambda})cos(\omega_0)sin(\omega_0|n|)) \quad (2)$$

where ω_0 and λ are respectively the spatial frequency and the spatial extension of the function $h^{(2)}(n)$, and C is a normalization constant. The function $h^{(2)}(\cdot)$ can be considered an intrinsic characteristic of the lattice network providing a computational primitive, the "Perceptual Engine", which can be used to obtain more powerful image descriptors e.g., Gabor-like functions [12].

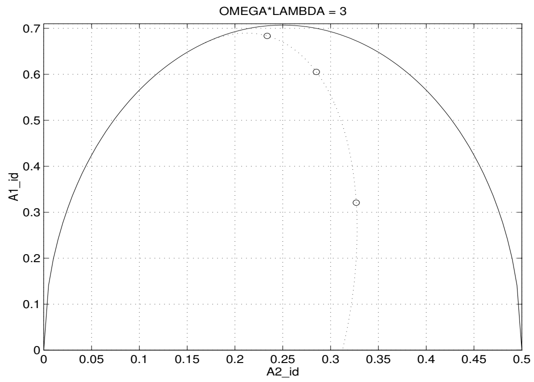

Fig. 1. Perceptual engine stability region (solid line). The dotted line represents the locus of the impulse responses with the same number of lobes: $\lambda\omega_0 = 3$ (see also below Fig. 3)

B. Transconductor-based implementation

The circuital interpretation of the lattice network difference equation can be obtained by letting:

$$e(\cdot) = \frac{V(\cdot)}{V_{ref}} \quad , \quad \frac{b_0}{a_0}s(\cdot) = \frac{I_s(\cdot)}{I_{ref}}$$

in Eq.(1), so obtaining:

$$A_2V_{n-2} - A_1V_{n-1} + V_n - A_1V_{n+1} + A_2V_{n+2} = \frac{V_{ref}}{I_{ref}}I_s(n) \quad (3)$$

where $I_s(n)$ is the photosensors input current whereas the output signal of the perceptual microsystem is the 1-D distribution of the node voltages V_n. Again, substituting:

$$G_{m,3} = \frac{I_{ref}}{V_{ref}} \quad , \quad G_{m,i} = A_i\, G_{m,3} \quad (4)$$

the final form of eq.(3) is:

$$G_{m,2}V_{n-2} - G_{m,1}V_{n-1} + G_{m,3}V_n + \\ -G_{m,1}V_{n+1} + G_{m,2}V_{n+2} = I_s(n) \quad (5)$$

Eq.(5) provides the electric modelling of the perceptual microsystem by connections of linear Voltage Controlled Current Sources (VCCSs). Fig. 2a shows the electric realisation of the single node of the lattice network by 3 linear transconductors whose transconductances, $G_{m,i}$, is

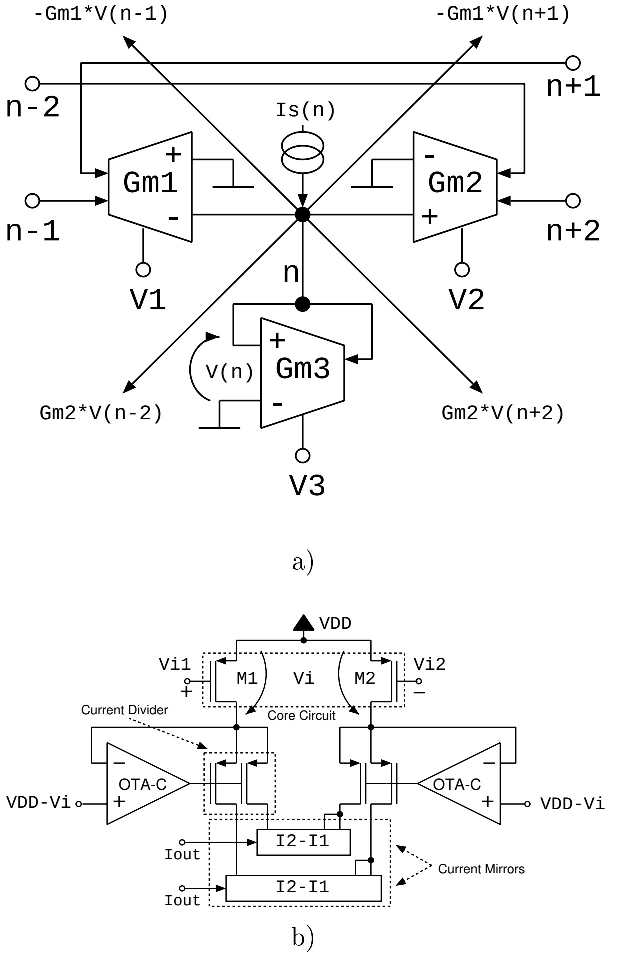

Fig. 2. Electric model of the node 1-D lattice network: a)structure of the n-th node, b)CMOS realisation of the tunable transconductor. Every MOS transistor has the source connected to its own well

function of an external tuning voltage V_i (for i=1,2 and 3). In it, transconductors $G_{m,1}$ and $G_{m,2}$ perform the interaction with the neighbor nodes whereas $G_{m,3}$ performs the local I/V conversion. Eq.(4) provide the G_m-based definition of the coefficient $\underline{A}$ as (for i=1,2):

$$\underline{A} = (A_1, A_2) = (\frac{G_{m,1}}{G_{m,3}}, \frac{G_{m,2}}{G_{m,3}}) \quad (6)$$

The above relation states that a perceptual microsystem tunable over any point inside of the elliptic region in Fig. 1 can be designed by adjusting the transconductances $G_{m,i}$ (for i=1,2) regarding $G_{m,3}$ as a design parameter.

Thus, linear tunable transconductor is the basic building block featuring the realisation of the perceptual engine. According to Eq.(6), in order to improve the accuracy of the coefficient $\underline{A}$ all the transconductors must exploit the same circuital realisation such that transconductance $G_{m,i}$ depends upon a minimal number of MOS transistor parameters.

C. CMOS tunable transconductor

1) Operation principle: The general scheme of the transconductor to be used in the realisation of the perceptual microsystem is shown in Fig. 2b. Assuming ideal OpAmp as well as current mirroring, the operation of the transconductor is obtained considering its core circuit represented by two equally sized pMOS transistors M1 and M2. They are biased in triode region with the same drain-source voltage, the tuning voltage V_i, and linear output current is obtained considering the difference between their drain current[13]. Thus, for i=1,2 and 3:

$$I_{out} = \frac{1}{2}(Id_2 - Id_1) = G^{id}_{m,i} Vd \tag{7}$$

where $Vd = V_{i1} - V_{i2}$ is the differential input voltage and $G^{id}_{m,i} = 0.5KV_i$ the voltage tunable transconductance. Substituting Eq.(7) into Eq.(6) yelds:

$$\underline{A}_{id} = (A_{1,id}, A_{2,id}) = (\frac{V_1}{V_3}, \frac{V_2}{V_3}) \tag{8}$$

where the condition $V_3 > V_i \geq 0$ must be respected. Relation (8) shows that wide-range tuning over the whole elliptic region can be obtained by varying the tuning voltage V_i (for i=1,2) regarding V_3 as a design parameter.

2) Analysis of Non-idealities: The analysis presented in the previous section does not take into account MOS transistor non-idealities. However, MOS transistor second-order behaviour as well as mismatch effects lead to deviations from the position $\underline{A}_{id}$. Thus, each non-ideality can be related to an error $\underline{\varepsilon}_n$ defined as the difference between the actual $\underline{A}_n$ and the adjustable position $\underline{A}_{id}$ as:

$$\underline{\varepsilon}_n = \underline{A}_n - \underline{A}_{id} \tag{9}$$

where $\varepsilon_{i,n} = A_{i,n} - A_{i,id}$ is the component of $\underline{\varepsilon}_n$ along the $A_{i,id}$-axes. The module of the error is:

$$\varepsilon_n = \sqrt{(A_{1,n} - A_{1,id})^2 + (A_{2,n} - A_{2,id})^2} \tag{10}$$

Perceptual microsystem non-idealities can be distinguished in: *systematic* and *node-dependent*. The first, lead to systematic node-independent errors which can be removed by properly adjusting the tuning voltages V_i in order to reach the position $\underline{A}_{id}$. The second class concerns error sources which have a strong influence on the output of the lattice network since its behaviour relies upon *symmetric cooperative interactions between neighboring nodes*. Thus, according to [14], node-dependent non-idealities should not affect the values local coefficients $\underline{A}_n$ more than 1% of their absolute values. - *Systematic errors* -

In a first-order approximation, both vertical field mobility reduction and parasitic Source/Drain resistances influence MOS drain current reducing its current factor K as $1/(1+\theta(Vgs - Vto))$. Each node of the lattice network interacts with the neighboring one by a local I-to-V-to-I conversion. Analogously to what happens in the simple current mirror, this K-reduction has not any influence on the actual value of the coefficient $\underline{A}_{id}$. Transistors M1 and M2 are biased at the same drain-source voltage, the module of V_i. Assuming a first-order modelling of the velocity saturation effect, the transconductance $G_{m,i}$ can be written as $G_{m,i} = G^{id}_{m,i}/(1 + V_i/(E_{sat}L))$, where L is their effective lengt. Thus, substituting Eq.(8) into Eq. (6) one obtains:

$$\underline{A} = (\frac{\beta_1 + A_{1,id}}{1+\beta_1}, \frac{\beta_2 + A_{2,id}}{1+\beta_2}) \tag{11}$$

if $\beta_i = \frac{V_3}{E_{sat}L} A_{i,id} \ll 1$ the following approximation holds:

$$\varepsilon \simeq \frac{V_3}{E_{sat}L}\sqrt{[(1-A_{1,id})A_{1,id}]^2 + [(1-A_{2,id})A_{2,id}]^2} \tag{12}$$

which predicts an error proportional to the ratio V_3/L. For $V_3/L = 1/10\ V/\mu m$ an error lower than 0.3% over each point in the elliptic domain can be obtained. Fig. 2b shows a 2-stages OpAmp connected as a voltage buffer imposing the biasing voltage V_i. Due to the finite loop gain A_{loop}, an error on the values of these drain-source voltages occurs. Accordingly, Eq.(6) can be rearrenged as:

$$\underline{A} = (\frac{1 + \frac{V_3}{V_{DD}} A_{loop} A_{1,id}}{1 + \frac{V_3}{V_{DD}} A_{loop}}, \frac{1 + \frac{V_3}{V_{DD}} A_{loop} A_{2,id}}{1 + \frac{V_3}{V_{DD}} A_{loop}}) \tag{13}$$

Thus, the error is:

$$\varepsilon = \frac{\sqrt{(1-A_{1,id})^2 + (1-A_{2,id})^2}}{1 + \frac{V_3}{V_{DD}} A_{loop}} \tag{14}$$

which is proportional to $A_{loop}V_{DD}/V_3$. For $V_3 = 1V$ and $A_{loop} = 500$ an error lower than 0.7% is obtained. Due to the non-zero transconductor output conductance $G_{0,i}$ a parasitic node conductance $G^n_0 = 2G_{0,1} + 2G_{0,2} + G_{0,3}$ is added to $G^{id}_{m,3}$ leading to an error in the local I/V conversion. Then, the coefficient $\underline{A}$ can be written as:

$$\underline{A} = (\frac{A_{1,id}}{1 + \frac{G^n_0}{G^{id}_{m,3}}}, \frac{A_{2,id}}{1 + \frac{G^n_0}{G^{id}_{m,3}}}) \tag{15}$$

where, if $\frac{G^n_0}{G^{id}_{m,3}} \ll 1$, the following approximation holds:

$$\varepsilon \simeq \frac{G^n_0}{G^{id}_{m,3}} \sqrt{A^2_{1,id} + A^2_{2,id}} \tag{16}$$

For a cascoded current mirror, assuming ideal OpAMps, $G^n_0/G^{id}_{m,3}$ is proportional to $1/L^2$ [15]. Using $L = 20\mu m$ an error lower than 0.04% can be obtained. - *Node-dependent errors* - Mismatch is the dominating node-dependent non-ideality. The effect of the mismatch on the performances of the perceptual microsystem is analised considering its influence on the behaviour of the transconductors. Accordingly, the transconductance can be written as $G_{m,i} = 0.5\tilde{K}V_i$ where $\tilde{K}$ is the current factor of the MOS transistor (M1 or M2) performing the V-to-I conversion. Thus, exploiting Eq.(6) one obtains:

$$\underline{A}_n = (\frac{1 + \frac{1}{2}(\frac{\delta K}{K})_{c,1}}{1 - \frac{1}{2}(\frac{\delta K}{K})_{c,1}} A_{1,id}\ , \frac{1 + \frac{1}{2}(\frac{\delta K}{K})_{c,2}}{1 - \frac{1}{2}(\frac{\delta K}{K})_{c,2}} A_{2,id}) \tag{17}$$

where $\delta K = \tilde{K} - K_1$ and $K = (\tilde{K} + K_1)/2$. The above relation states that coefficient accuracy is related to the matching properties between the MOS transistors performing the V-to-I conversion. Several other contributions to the mismatch must be considered in the expression of the overall error (10). Current mismatch occurring in the mirrors $(\frac{\delta I}{I})_m$ as well as in MOS current dividers $(\frac{\delta I}{I})_d$ increase the error on the position $\underline{A}_{id}$. OpAmp's offset voltage V_o adds to the bias voltage V_i, a mainly random voltage shift, thus enlarging the overall error. Taking into account these effects, a general expression for the coefficients $A_{i,n}$ is:

$$A_{1,n} = \frac{1+\frac{1}{2}(\frac{\delta K}{K})_{c,1}}{1-\frac{1}{2}(\frac{\delta K}{K})_{c,1}} \frac{V_1 A_{1,id} + V_{o,1}}{V_3 + V_{o,3}} \frac{1+(\frac{\delta I}{I})_{d,1}}{1+(\frac{\delta I}{I})_{d,3}}(1+(\frac{\delta I}{I})_m)$$

$$A_{2,n} = \frac{1+\frac{1}{2}(\frac{\delta K}{K})_{c,2}}{1-\frac{1}{2}(\frac{\delta K}{K})_{c,2}} \frac{V_2 A_{2,id} + V_{o,2}}{V_3 + V_{o,3}} \frac{1+(\frac{\delta I}{I})_{d,2}}{1+(\frac{\delta I}{I})_{d,3}}$$

Assuming independent random variables, an estimation of the error is $\varepsilon_{n,max} = \sqrt{\sigma_1^2 + \sigma_2^2}$ where,

$$\sigma_1^2 = [\sigma_c^2(\frac{\delta K}{K}) + \sum_{i \in \{1,3\}} \sigma_{d,i}^2(\frac{\delta I}{I}) + \sigma_m^2(\frac{\delta I}{I})]A_{1,id}^2 + \frac{\sigma^2(V_o)}{V_3^2}(1+A_{1,id}^2)$$

$$\sigma_2^2 = [\sigma_c^2(\frac{\delta K}{K}) + \sum_{i \in \{2,3\}} \sigma_{d,i}^2(\frac{\delta I}{I})]A_{2,id}^2 + \frac{\sigma^2(V_o)}{V_3^2}(1+A_{2,id}^2)$$

For $\underline{A}_{id} = \underline{0}_{id}$ the error reaches a mininum proportional to $\sigma(V_o)/V_3$. Exploting proper MOS sizing ($L_c = W_c = 15\mu m, L_d = W_d = L_m = W_m = 30\mu m$ and $V_3 = 1V$) and low offset design technique an error lower than 0.5% has been obtained, for a wide variation range of $\underline{A}_{id}$.

In order to quantify the influence of the mismatch on the simmetry of the cooperative interactions of the lattice network, the definition of the error (9) must be changed as: $\underline{\varepsilon}_{n,k} = \underline{A}_n - \underline{A}_k$. By adding and subtracting the voltage ratio $\underline{A}_{id}$ this error can be rewritten as: $\underline{\varepsilon}_{n,k} = \underline{\varepsilon}_n - \underline{\varepsilon}_k$ which gives the dependence upon the error defined in Eq.(9). Thus, still assuming a statistical independence among the parameters of devices belonging to different nodes, a σ-estimation of the maximun error is:

$$\varepsilon_{n,k}^{max} = \sqrt{[\sigma(\varepsilon_{1,n}) + \sigma(\varepsilon_{1,m})]^2 + [\sigma(\varepsilon_{2,n}) + \sigma(\varepsilon_{2,m})]^2} = 2\varepsilon_{max} \qquad (18)$$

which is in agreement with [14] where it is assumed that only the mismatch between the neighbor and the next neighbor nodes is meaningful.

3) Temperature sensitivity: The analysis on temperature dependence of the perceptual microsystem is carried out by considering Eq.(6). In it coefficient $\underline{A}_n$ is defined as the transconductances ratio at the selected node of the lattice network. Thus, in a first-order approximation, temperature variation of these coefficients is mainly related to the temperature dependence on the ratio between the mobilities of the local MOS transistors performing the V-to-I conversion. Therefore, by properly matching these MOSs, an almost temperature insensitive perceptual microsystem can be obtained.

D. Results

We considered a perceptual microsystem composed of 64 nodes designed for the CMOS 2.5μ N-well MIETEC process. We analysed its performance through extensive HSpice simulations. In Fig. 3 the output voltage for three different pairs of the interaction parameters are shown. Their values are chosen to obtain filters (percetual engines) of different spatial frequencies, but with the same number of lobes (sidebands). The results are well in agreement with what espected by the analitical model.

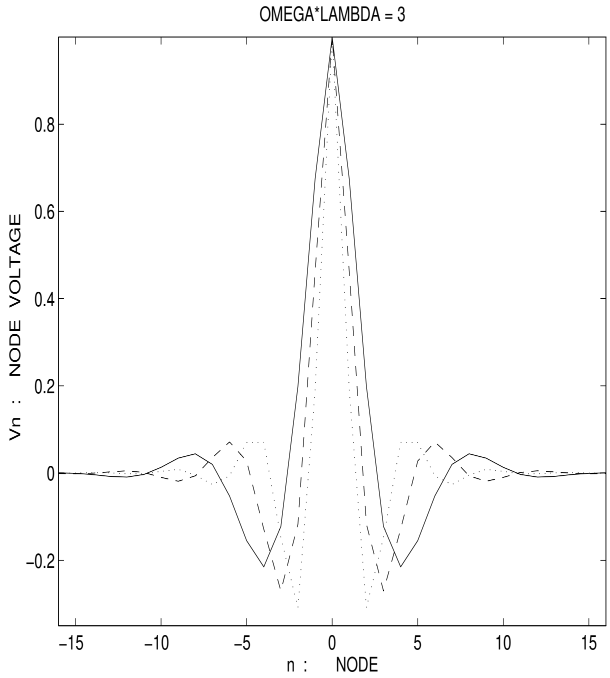

Fig. 3. Normalised node voltage distributions for three pairs of (A_1, A_2) interaction coefficients with iso-lobes impulse response: $\lambda\omega_0 = 3$. Considering $V_3 = 1V$ and $V_{DD} = -V_{SS} = 2.5V$, the selected points $\underline{A}_{id} \in \{(0.32, 0.33), (0.61, 0.29), (0.68, 0.23)\}$, corresponding to the following pairs of filter parameters $(\omega_0, \lambda) \in \{(\pi 3/7, 7/\pi), (\pi/3, 9/\pi), (\pi/4, 12/\pi)\}$, see Fig. 1.

III. System solutions and applications

In this section, we'll examine the application capabilities of our perceptual microsystem as a front-end module in a machine vision system, describing in detail its potential application in stereoscopic depth perception and , in perspective, in motion analysis. 64 1-D node arrays are placed in rows and receive the excitation signals from sensor outputs (see Fig. 4). The filtering action occurring through convolution with the perceptual engine kernel is controlled in frequency and spatial extension by adjusting the potentials V_1, V_2, and V_3. Each row is scanned column-wise combining the excitatory signals of three neighboring cells, to obtain the convolution of the input image with odd and even Gabor-like kernels. The outputs OGC and EGC are fed to a processing module (see Fig. 5) customized according to the specific early vision task to be performed (e.g., the stereoscopic depth estimation described below).

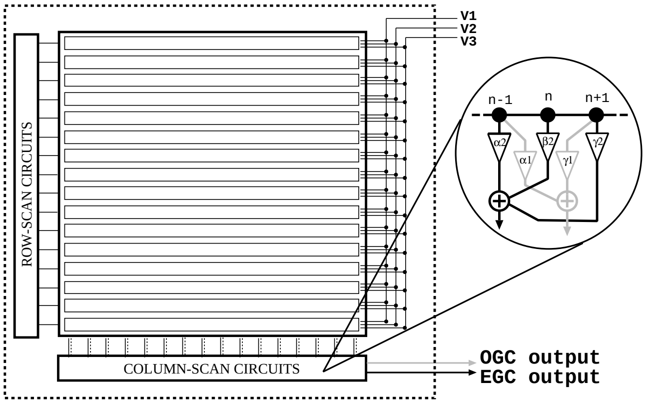

Fig. 4. The perceptual microsystem core: the column-scan circuits perform the weighted combination on neighboring node voltages, leading to the output signals OGC and EGC corresponding to the convolutions of the input image with odd and even Gabor-like filters, respectively. The supply lines of control voltages V_i used to tune each perceptual engine, are evidenced.

A. Stereo depth estimation

Stereoscopic depth estimation is mainly based on disparity measurement. Disparity is a local property that can be associated to a stereo pair (left and right) of images or image sequences. Hence, a joint representation of the information flows coming from the two eyes is a definitive need for stereoscopic depth perception. Such a joint representation can be related to the spatial properties of binocular filters tuned to specific disparity values. This problem has an elegant formulation in the frequency domain, in relation to the so-called phase-based matching methods [16]. Basically, disparity estimation is computed as the shift necessary to align the phase values of the band-pass filtered version of the binocular stereo signals. One can assume that the disparity between the stereo image pair occurs only along the direction of the epipolar lines. In the simplest configuration, in which optical axes are parallel, epipolar lines are parallel to the line joining the optical centers of the cameras. In such conditions, stereo phase-based matching can be casted as a 1D problem. The local phase is computed following Sanger's algorithm [16], from the output of a pair of Gabor filters in quadrature (see Fig. 6). The differential measure of the local phase, obtained by the left and right retinas, is validated by a confidence measure, thus deriving a reliable

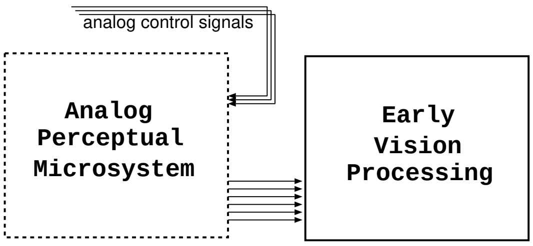

Fig. 5. General scheme for a machine vision system based on the perceptual microsystem module.

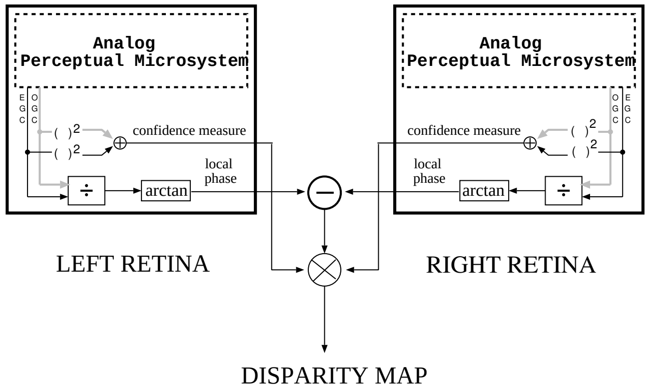

Fig. 6. Schematic representation of the architecture of the stereo depth perception system.

disparity map. In Fig. 7 the image reproduces a simple toy-car reconstruction of a traffic/vehicle scene. The disparity map, obtained through a simulation of the system depicted in Fig. ??, evidences in light gray the car closer to the viewer, and in darker gray the approaching car in the background.

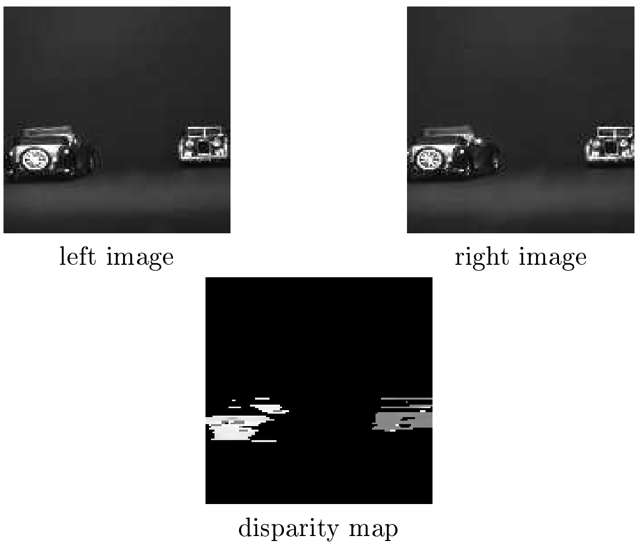

Fig. 7. Example of depth estimation from a stereo image pair. The disparity map, obtained through a simulation of the system depicted in Figs. 4-5, evidences in light gray the car closer to the viewer, and in darker gray the approaching car in the background.

B. Motion analysis

Several approaches to motion analysis rely upon correspondence measures in the spatio-temporal domains of a visual scene. Among the others, the so-called "energy" or "spatio-temporal" models [17] are based on a linear filtering operation with kernels with a specific orientation in the spatio-temporal plane which gives them a specific direction sensitivity. A set of such filters are often used as a first stage of motion algorithms in order to extract information about local velocity [18].

Adelson and Bergen [17] demonstrated that spatio-temporal oriented filters can be constructed from pairs of separable (i.e., not oriented) filters. According to the method of Adelson and Bergen, filters tuned to specific directions can be obtained through a temporally modulated combination of perceptual engines. Specifically, by taking appropriate sums and differences of the outputs of a 2nd-order lattice network, it is possible to construct pairs of spatio-temporal oriented filters to be used to measure and discriminate the energy of motion. For example, an even filter sensitive to leftward motion can be obtained with the following combination of the perceptual engine responses:

$$\begin{aligned} g_{LE} = \alpha_{odd} f_3(t)h(n-1) + \gamma_{odd} f_3(t)h(n+1) + \\ \alpha_{even} f_5(t)h(n-1) + \beta_{even} f_5(t)h(n) + \\ +\gamma_{even} f_5(t)h(n+1) \end{aligned} \quad (19)$$

where f_3 and f_5 are modulating functions temporally in quadrature.

IV. Conclusions

The approach followed in this paper can be related to the research path followed by Carver Mead and his co-workers [19] towards efficient silicon implementations of visual tasks. VLSI cooperative networks are seen both as a medium whose structure is in many ways similar to neural structures [20] [21], and as the circuit analogue of the discretized forms of machine vision algorithms [22]. The main innovative feature of our approach concerns (i) the architectural specification of an analog perceptual agent –the *perceptual engine*– to be used as a powerful building block for early vision perceptual tasks; (ii) the VLSI implementation of such recurrent network as an analog CMOS circuit, based on continuously adjustable interactions parameters.

The perceptual applications presented focus on low-level vision tasks such as extraction of stereo disparity, and analysis of motion. In perspective, information processing capabilities at intermediate and high levels could be obtained using our microsystem and adding further processing layers of similar cells.

References

[1] J.J. Koenderink. Scale-time. *Biol. Cybern.*, 58:159–162, 1988.

[2] H. Wechsler. Multiscale and distributed visual representations and mappings for invariant low-level perception. In H. Wechsler, editor, *Neural Networks for Perception I*, pages 462–476. Academic Press, 1992.

[3] F. Farrokhnia. *Multi-channel filtering techniques for texture segmentation and surface quality inspection.* PhD thesis, Hielipan State University, 1990.

[4] J.J. Kulikowski, S. Marčelja, and P.O. Bishop. Theory of spatial position and spatial frequency relations in the receptive fields of simple cells in the visual cortex. *Biol. Cybern.*, 43:187–198, 1982.

[5] J.G. Daugman. Uncertainty relation for resolution in space, spatial frequency, and orientation optimized by two-dimensional visual cortical filters. *J. Opt. Soc. Amer.*, A/2:1160–1169, 1985.

[6] D. Marr. *Vision.* New York: Freeman, 1982.

[7] I. Fogel and D. Sagi. Gabor filters as texture discriminator. *Biol. Cybern.*, 61:103–113, 1989.

[8] W.T. Freeman and E.H. Adelson. The design and use of steerable filters. *IEEE Trans. Pattern Anal. Mach. Intell.*, 13(9):891–906, 1991.

[9] T. Poggio, V. Torre, and C. Koch. Computational vision and regularization theory. *Nature*, 317:638–643, 1985.

[10] L. Raffo, S.P. Sabatini, G.M. Bo, and G.M. Bisio. Visual perception microsystems based on distributed analog VLSI processing. In *Proc. 2nd Int. Workshop on Mechatronical Computer Systems for Perception and Action, MCPA'97*, pages 13–21, Pisa, Italy, February 1997.

[11] L. Raffo. Analysis and synthesis of resistive networks for distributed visual elaborations. *Electronics Letters*, 32(8):743, April 1996.

[12] S.P. Sabatini, L. Raffo, F. Solari, A. Bonfiglio, and G.M. Bisio. Smart materials for visual perception. In *EAEC'97 Congress, Conference IV "Advanced Automotive Electronics"*, pages 871–879, Cernobbio, Italy, July 1997.

[13] Y. Tsividis, Z. Czarnul, and S.C. Fang. MOS transcondactors and integrators with high linearity. *Electronics Letters*, 22:245–246, 1986.

[14] L. Raffo. Resistive network implementing maps of Gabor functions of any phase. *Electronics Letters*, 31(22):1913–1914, 1995.

[15] Z. Wang. Analytical determination of output resistance and DC matching errors in MOS current mirrors. *IEE Proceedings-G*, 137:397–404, October 1990.

[16] T.D. Sanger. Stereo disparity computation using Gabor filters. *Biol. Cybern.*, 59:405–418, 1988.

[17] E.H. Adelson and J.R. Bergen. Spatiotemporal energy models for the perception of motion. *J. Opt. Soc. Amer.*, 2:284–321, 1985.

[18] S.J. Nowlan and T.J. Sejnowski. Filter selection model for motion segmentation and velocity integration. *J. Opt. Soc. Amer.*, 11:3177–3200, 1994.

[19] C.A. Mead. *Analog VLSI and Neural Systems.* Addison-Wesley, Reading, 1989.

[20] M.A. Sivilotti, M.A. Mahowald, and C.A. Mead. Real-time visual computations using analog CMOS processing arrays. In *Advanced Research in VLSI:Proc. Stanford Conference 1987*, pages 295–312, 1987.

[21] C.A. Mead and M.A. Mahowald. A silicon model of early visual processing. *Neural Networks*, 1:91–97, 1988.

[22] C. Koch. Seeing chips: Analog VLSI circuits for computer vision. *Neural Comp.*, 1:184–200, 1989.